eXPRESS Polymer Letters Vol.3, No.4 (2009) 219–225
Available online at www.expresspolymlett.com
DOI: 10.3144/expresspolymlett.2009.28

New fluorescent polymeric nanocomposites synthesized by antimony dodecyl-mercaptide thermolysis in polymer

F. Capezzuto[1], G. Carotenuto[1], F. Antolini[2], E. Burresi[2], M. Palomba[1], P. Perlo[3]*

[1]Institute of Composite and Biomedical Materials, P.le Tecchio, 80 – 80125 Napoli, Italy
[2]ENEA Research Center of Faenza, Dept. of Advanced Physical Technologies and New Materials Via Ravegnana 186 – 48018 Faenza (Ra), Italy
[3]FIAT Research Center, Strada Torino 50 – 10043 Orbassano (TO), Italy

Received 5 January 2009; accepted in revised form 21 February 2009

Abstract. In this work, the formation of semiconductive Sb_2S_3 nanoparticles inside amorphous polystyrene has been achieved by thermal degradation of the corresponding antimony dodecyl-mercaptide, $Sb(SC_{12}H_{25})_3$. The thermolysis of the dodecyl-mercaptide precursor was studied as both pure phase and mercaptide solution in polystyrene. The thermal decomposition of the antimony mercaptide precursor at 350°C, under vacuum, showed the formation of a mixture of antimony trisulfide (stibnite, Sb_2S_3) and zero-valent antimony (Sb) phase. X-ray Powder Diffraction (XRD) and Rietveld analysis carried out on the obtained nanostructured powder confirmed the presence of Sb and Sb_2S_3 phases in 10.4 wt% and 89.6 wt% amount, respectively. The same pyrolysis reaction was carried out in the polymer and the resulting nanocomposite material was characterized by X-ray diffraction (XRD), transmission electron microscopy (TEM), UV-VIS spectroscopy, and fluorescence spectroscopy. The nanocomposite structural characterization indicated the presence of well-dispersed nanoclusters of antimony and stibnite (15–30 nm in size) inside the amorphous polymeric phase. Optical measurements on the obtained nanocomposite films showed a strong emission at 432 nm upon excitation at 371 nm, probably related to the presence of Sb_2S_3 nanoclusters.

Keywords: *nanocomposites, stibnite, antimony, mercaptide, fluorescence*

1. Introduction

Polymer nanocomposites made of nanoparticles (spheres, rods, plates, etc.) embedded into a polymeric matrix extend the potentialities of polymers while maintaining the manufacturing and processing flexibility inherent to plastics [1–6]. In fact, the potential impact of polymeric nanocomposite materials lies in the synergistic combination of nanoparticles and polymers properties that can lead not only to the sum of the organic and inorganic phase characteristics, but also to new functionalities with respect to the single materials [6–9]. The advantages of these materials arise mainly from the filler size reduction to nanoscale, considering that the concomitant quantum confinement effects induce new physical phenomena [10, 11]. In fact, nanoparticles have unique optical and electronic properties not observed in the corresponding bulk materials [12, 13].

As already said, it is well known that the embedding of nanoscale fillers into a polymeric matrix offers the possibility to achieve materials with properties combination not realizable by the single components. In particular, the combination of fluorescent semiconductor nanoparticles with optical polymers yields to a new class of materials characterised by both fluorescence and transparency characteristics. The luminescent properties of semicon-

*Corresponding author, e-mail: giancaro@unina.it

ductor nanoparticles stem from the separation of the conductive and valence band due to the quantum-size effect. Nowadays, the luminescent properties of semiconductor nanoparticles are thoroughly studied for the development of new labelling systems for biomedical purposes [14] and for light-emitting devices applications [15–17]. Especially in the last case, the combination of nanoparticles and polymers is of special interest because the mechanical and electro-optical properties of polymers joined with the high stability of nanoparticles as light-emitters allow the set-up of industrially competitive systems for light-source production.

Antimony trisulfide, Sb_2S_3 is an interesting material, with unique optical properties and currently under study as potential photovoltaic material [18, 19]. Sb_2S_3 is a semiconductor which has been also studied for its high photosensitivity and thermoelectric power [20]. It has been used in television cameras with photoconducting targets, microwave devices, thermoelectric, electronic and optical devices, as well as in infrared (IR) spectroscopy [21]. The optical properties of the Sb-Sb_2S_3 system were studied by fluorimetry since this material shows photoluminescence characteristics [22]. In addition, sphere-like nanomaterials have excellent optical, physical and chemical properties that could be widely applied in biology, as fluorescence probes [23–25].

In this work, the synthesis of luminescent stibnite-antimony, Sb_2S_3-Sb, nanoparticles embedded into a polymer matrix, by thermolysis of antimony dodecyl-mercaptide, $Sb(SC_{12}H_{25})_3$, dissolved in polymer is reported. It has been shown that the thermal decomposition of mercaptides is a powerful synthesis method for a number of noble metals, semimetals and metal sulphide [26]. Sb_2S_3 nanomaterials can be synthesised by several methods namely hydrothermal method, refluxing polyol process, or in solution at room temperature, however the proposed synthesis allows the material preparation at quite mild temperature conditions (150–250°C), absolutely compatible with the thermal stability of common polymers. Here, the structural and morphological characteristics of the $Sb(SC_{12}H_{25})_3$ thermolysis product and the luminescent behaviour of the Sb_2S_3-Sb/polystyrene system are given.

2. Experimental

Antimony dodecyl-mercaptide, $Sb(SC_{12}H_{25})_3$, was prepared by adding drop-by-drop an alcoholic solution of dodecanethiol, $C_{12}H_{25}SH$ (Aldrich), to an antimony chloride solution, $SbCl_3$ (Aldrich, 99.9%) in ethanol (Fluka, 99.8%) at room-temperature, under stirring (see Equation (1)) [27]. Stoichiometric amounts of reactants were used. The mercaptide precipitation did not take place after reactants mixing, but a pH correction, by addition of ammonium hydroxide, $NH_3{\cdot}H_2O$ (Aldrich) was required (see Equation (2)). The mercaptide promptly precipitated in form of a white crystalline powder, which was separated by vacuum-filtration and then washed several times with ethanol. The antimony dodecyl-mercaptide was further purified from the NH_4Cl by-product by dissolution in chloroform followed by filtration and solvent evaporation (Equations (1) and (2)):

$$SbCl_3 + 3C_{12}H_{25}SH \rightleftharpoons Sb(SC_{12}H_{25})_3 + 3HCl \quad (1)$$

$$HCl + NH_4OH \rightarrow NH_4Cl + H_2O \quad (2)$$

The thermal decomposition of the obtained antimony dodecyl-mercaptide at 350°C, under vacuum (2 mbar), by using a hotplate, is expected to give an inorganic product made of a mixture of stibnite, Sb_2S_3, and antimony, Sb, powders. A preliminary study of the mercaptide thermal degradation has been carried out by Differential Scanning Calorimetry (DSC-TA Instruments 2920) from room-temperature to 150°C, at 10°C/min, under fluxing nitrogen, using sealed aluminium capsules. From the DSC and X-ray Powder Diffraction analysis of the inorganic powder product of the antimony dodecyl-mercaptide pyrolysis, it results that the processes developed during the thermal treatment took place in the following steps: (i) mercaptide melting at ca. 50°C, (ii) mercaptide decomposition to nanometric antimony (Sb) and antimony sulfide (Sb_2S_3) at ca. 150°C, and (ii) evaporation of the organic by-products, which refluxed inside the flask at ca. 300°C. After cooling down at room temperature, the inorganic phase was washed by chloroform and separated by centrifugation at 8000 rpm for 10 minutes.

In order to obtain stibnite-antimony/polystyrene nanocomposite films, $Sb(SC_{12}H_{25})_3$ was dissolved in chloroform and mixed with a chloroform solution of polystyrene (Aldrich, molecular weight

M_w = 230 000 gmol^{-1}). $Sb(SC_{12}H_{25})_3$/polystyrene blend consisting of 5% by weight of mercaptide component was prepared. The obtained system was cast onto a glass-substrate and allowed to dry at room temperature. The thermal annealing of the obtained $Sb(SC_{12}H_{25})_3$/polystyrene blend was performed at ca. 250°C, using a hot-plate, and it led to stibnite-antimony/polystyrene nanocomposite film. Both powder and nanocomposite films were investigated by X-ray Powder Diffraction (XRD). The Sb_2S_3-Sb powder (hand ground in an agate mortar) was loaded in an aluminium flat holder and the X-ray data were collected using a Philips conventional Bragg-Brentano vertical diffractometer with Cu-K_α radiation. The investigated 2Θ range was 5–80° in steps of 0.02° and 8 s per step. The phase identification was carried out by means of X' pert High Score software (data base ICDD PDF2 Sets 1-82). The observed data were refined with GSAS (Larson and Von Dreele). The nanocomposite film was investigated in the 2Θ range from 5 to 80° with a step size of 0.02° and 1 s per step by means of a Rigaku DMAX-IIIC, using Cu-K_α radiation, λ = 1.5418 Å.

The morphology of the Sb_2S_3-Sb powder mixture was examined by Scanning Electron Microscopy (SEM, Cambrige-S360) and the $Sb(SC_{12}H_{25})_3$/polystyrene nanocomposite film was investigated by Transmission Electron Microscopy (Philips EM208S microscope equipped with a MegaView Camera for digital imaging, using an accelerating voltage of 100 kV) and photoluminescence spectroscopy (Perkin-Elmer-LS55 spectrofluorometer using a pulsed xenon lamp as an excitation source). TEM specimens were prepared by dissolution of the nanocomposite material in chloroform and the obtained solution was cast on graphitized film supported on copper mesh grids.

3. Results and discussion

The DSC thermogram of pure $Sb(SC_{12}H_{25})_3$ shows an endothermic peak at 48°C, corresponding to the antimony dodecyl-mercaptide melting point. The nature of the inorganic products resulting from $Sb(SC_{12}H_{25})_3$ pyrolysis was investigated by X-ray Powder Diffraction (see Figure 1). In order to obtain an accurate and quantitative phase analysis, a Rietveld refinement was performed. Two main phases were identified: stibnite (Sb_2S_3, reference pattern N° 01-073-0393 crystal system Orthorhombic, space group Pnma, crystal lattice parameters a = 11.3107 Å, b = 3.8363 Å, c = 11.2285 Å, V = 487.22 Å^3) and antimony (Sb, reference pattern N° 01-085-1324, crystal system Rhombohedral, space group R-3m, crystal lattice parameters a = 4.3007 Å, b = 4.3007 Å, c = 11.2220 Å, V = 179.75 Å^3). A preliminary quantization of the two component amounts in the investigated powder mixture, carried out using the RIR ratio, displays 95 wt% stibnite and 5 wt% antimony. However, a more sophisticate phase quantization was carried out by using the Rietveld method with the GSAS program. The final agreement factors of the Rietveld refinement for the investigated stibnite/antimony mixture are R_{wp} = 16.7%, R_p = 12.9% and χ^2 = 1.6, with a phase estimation of 10.4 wt% Sb and 89.6 wt% Sb_2S_3. The refinement lattice parameters of these phases are: stibnite a = 11.3103 Å, b = 3.8367 Å, c = 11.2289 Å, V = 487.27 Å^3 and antimony a = 4.3073 Å, b = 4.3073 Å, c = 11.2752 Å, V = 181.16 Å^3. The result of the Rietveld method was obtained refining the background, both cells, profiles, intensities and orientation. As it can be seen, the calculated lattice crystal parameters of stibnite are in good agreement with the observed one, while the calculated lattice parameters of antimony are slightly higher with respect to the expected ones. Both methods show

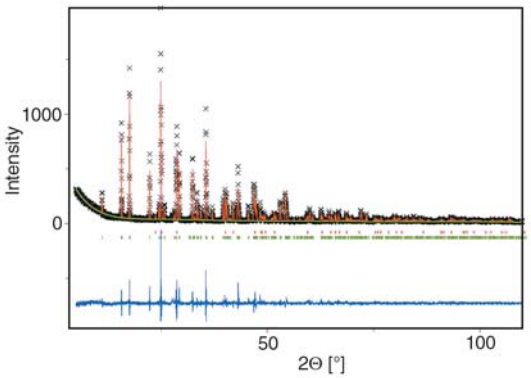

Figure 1. XRD pattern of the inorganic powder resulting from the $Sb(SC_{12}H_{25})_3$ thermolysis at 350°C, under vacuum. The observed and calculated XRD patterns are reported as black cross and red line. The difference between the calculated and experimental spectra is reported as a blue line. The red bars are the peak's markers of the antimony while the green bars represent the stibnite.

a)

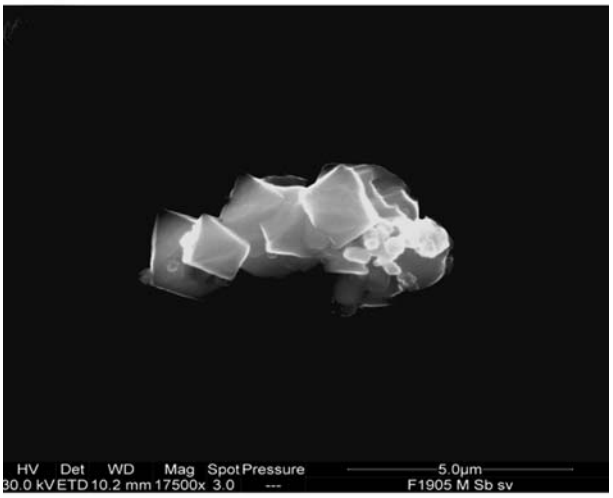

b)

Figure 2. Representative SEM micrograph of the powder product resulting from the $Sb(SC_{12}H_{25})_3$ thermolysis at 350°C, under vacuum: a) Sb_2S_3 prismatic crystals and b) Sb polyhedral crystals

that stibnite is the main phase, while the antimony is present only in small amount.

The SEM-micrograph of the inorganic phase Sb_2S_3/Sb (see Figure 2) shows two different solid phases: one, made of prismatic shaped crystals, corresponding to stibnite (Figure 2a) and the other one, made of aggregated polyhedral crystals, corresponding to zero-valent antimony (Figure 2b). The crystals size was evaluated from the SEM micrographies by image analysis using Sigma Scan Pro 5.0 and gave the following information: the prismatic stibnite crystals have a length ranging from 30 to 150 µm and ca. 10–20 µm in diameter, while the polyhedral antimony crystals have an average size of 2–3 µm.

After this preliminary study of pure antimony dodecyl-mercaptide thermal degradation, the mercaptide decomposition in polymer has also been investigated. The XRD pattern of stibnite-antimony/polystyrene nanocomposite film (see Figure 3) shows a broad reflection at ca. 20°, corresponding to the diffuse alone of amorphous polymer matrix and different peaks belonging to diffraction patterns of the inorganic nanostructured phase. The phase analysis of dodecyl-mercaptide decomposed in polystyrene allows the identification of two main phases: stibnite (Sb_2S_3, reference pattern N° 01-073-0393) and antimony (Sb, reference pattern N° 01-085-1324), just like in the case of pure dodecyl-mercaptide thermal decomposition.

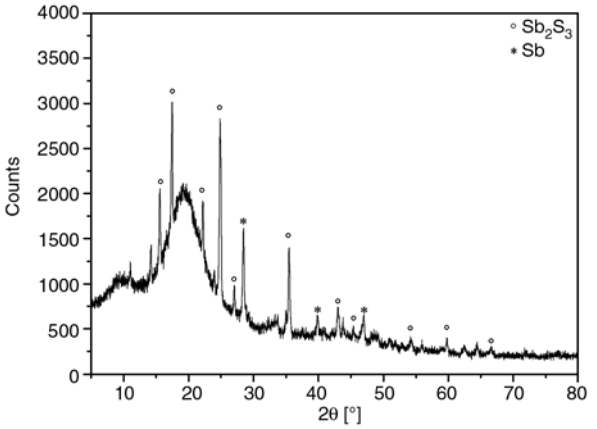

Figure 3. XRD pattern of the $Sb(SC_{12}H_{25})_3$/polystyrene blend thermally treated at 250°C

A representative TEM micrograph of the stibnite-antimony/polystyrene system is shown in Figure 4. TEM samples were prepared by dissolving 100 mg of nanocomposite in 20 ml of chloroform. A drop of the resulting solution was placed onto TEM copper grid support. As visible, the average size of the

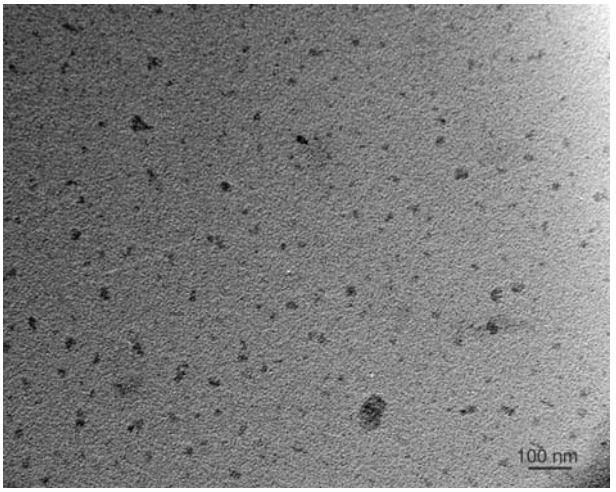

Figure 4. Typical TEM micrograph of the $Sb(SC_{12}H_{25})_3$/polystyrene thermally treated at 250°C

inorganic nanocrystals (stibnite and antimony clusters) was of ca. 15–30 nm.

The photoluminescence spectra of the nanocomposite antimony-stibnite/polystyrene films are shown in Figure 5. It can be seen that the excitation and emission peaks are shifted to higher wavelength values with respect to the corresponding peaks of the used pure polystyrene which exhibits a maximum of emission band at 389 nm for a maximum excitation at 296 nm. In fact, the emission band peak of the stibnite-antimony/polystyrene system appeared at 432 nm when excited at 371 nm which is the maximum of the absorption spectrum (see Figure 5). These spectra show a shape similar, to that of organic luminescent dyes, because the excitation and emission spectra result quite symmetric (mirror-like shaped peaks) [14]. This feature is rarely observed with nanoparticles, since nanocrystals usually exhibit a broad absorption with a narrow symmetric photoluminescence spectra (full-width at half maximum of 25–40 nm) [14]. The presence of the tail in the emission spectrum of the nanocomposite can be explained by taking into account the size distribution and the not uniform shape of the nanoparticles inside the polymer producing different emission spectra. As reported by other authors [28–30], the presence of surface traps, that modulates the emission of nanocrystals, should be also taken into consideration.

In order to exclude that the photoluminescence signal was related to the polystyrene presence, the emission spectrum of the nanocomposite was recorded at 296 nm, i.e. the excitation wavelength typical of polystyrene. As a result this experiment gives an emission signal with a maximum at 424 nm (data not shown). This photoluminescence band shows a lower intensity and a shift of the maximum with respect to the band of the nanocomposite obtained with λ_{exc} = 371 nm, excluding a possible role of the polystyrene matrix in the nanocomposite material photoluminescence. In addition, the approximate value of the nanocomposite energy band-gap ($E_g = hc/\lambda_{em}$) has been evaluated from the maximum emission peak wavelength in the PL spectra. The measured value of this energy band-gap is ca. 2.87 eV (λ_{em} = 432 nm) which is almost 1 eV higher than the Sb_2S_3 bulk-value (1.6 to 1.9 eV [31–32]). This result is in accordance with a well-known quantum-size effect observed with nanosized semiconductor materials [10, 11].

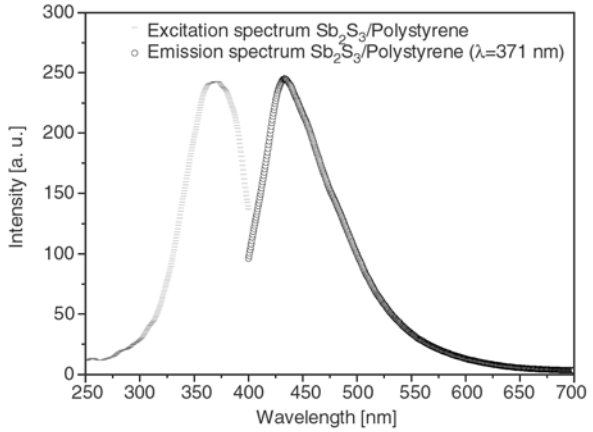

Figure 5. Photoluminescence spectra of an antimony-stibnite/polystyrene nanocomposite film

4. Conclusions

The antimony dodecyl-mercaptide thermolysis has been studied as a pure phase and as solution in polymer. In both cases the thermal decomposition of the mercaptide gave a mixture of antimony trisulfide (Sb_2S_3) and zero-valent antimony powder. The stibnite/antimony mixture obtained from the thermolysis of pure $Sb(SC_{12}H_{25})_3$ is made of 89.6 wt% Sb_2S_3 prismatic crystals (30–150 μm length and 10–20 μm in diameter) and 10.4 wt% of Sb aggregated polyhedral crystals (average size 2–3 μm). The antimony-stibnite/polystyrene nanocomposite, prepared by the thermolysis of $Sb(SC_{12}H_{25})_3$ dissolved in polystyrene, exhibits peculiar luminescent characteristics due to the stibnite nanocrystals with average dimensions ranging from 15 to 30 nm. The possibility to produce in situ polymer nanocomposites with new functionalities is of great importance for application in widespread fields and the here proposed synthesis method based on antimony dodecyl-mercaptide thermolysis in polystyrene is compatible with all current polymer manufacturing technologies.

Acknowledgements

The authors would like to thank to Prof. G. Artioli (Dipartimento di Mineralogia e Petrologia Università di Padova, Italia) and Dr. M. Dapiaggi (Dipartimento di Scienze della Terra 'Ardito Desio', Università di Milano I, Italia) for many stimulating discussions on XRD science.

References

[1] Carotenuto G., Nicolais L.: Nanocomposites, metal-filled. in 'Encyclopedia of Polymer Science and Technology' (ed.: Mark H. F.) Wiley, New York, Vol 10, 235–254 (2003).

[2] Mayer A. B. R.: Formation of noble metal nanoparticles within a polymeric matrix: Nanoparticle features and overall morphologies. Materials Science and Engineering: C, **6**, 155–166 (1998). DOI: 10.1016/S0928-4931(98)00049-6

[3] Carotenuto G., Nicolais L., Perlo P., Martorana B.: Method of production of polymer/metal or metal sulphide composites which uses metal mercaptides. U.S. Patent 7329700, USA (2007).

[4] Vecchione R., Carotenuto G., Casuscelli V., Esposito F., Leonardi S., Nicolais L., Volpe M. V.: Process for the preparation of a composite polymeric material. U.S. Patent 20060121262, USA (2006).

[5] Cardone G., Carotenuto G., Longo A., Perlo P., Ambrosio L.: Synthesis of gold nano-plates by mercaptide thermolysis in poly(vinyl acetate). Express Polymer Letters, **1**, 604–607 (2007). DOI: 10.3144/expresspolymlett.2007.82

[6] Caseri W.: Nanocomposites of polymers and metals or semiconductors: Historical background and optical properties. Macromolecular Rapid Communications, **21**, 705–722 (2000). DOI: 10.1002/1521-3927(20000701)21:11<705::AID-MARC705>3.0.CO;2-3

[7] Godovsky D. J.: Device applications of polymer-nanocomposites. Advances in Polymer Science, **153**, 163–205 (2000). DOI: 10.1007/3-540-46414-X

[8] Chen W., Joly A. G., Malm J. O., Bovin J. O., Wang S. J.: Full-color emission and temperature dependence of the luminescence in poly-*P*-phenylene ethynylene-ZnS/Mn^{2+} composite particles. The Journal of Physical Chemistry B, **107**, 6544–6551 (2003). DOI: 10.1021/jp034476r

[9] Šajinović D., Šaponjic Z. V., Cvjetićanin N., Marinović-Cincović M., Nedeljković J. M.: Synthesis and characterization of CdS quantum dots-polystyrene composite. Chemical Physics Letters, **329**, 168–172 (2000). DOI: 10.1016/S0009-2614(00)00990-8

[10] Gubin S. P., Kataeva N. A., Khomutov G. B.: Promising avenues of research in nanoscience: Chemistry of semiconductor nanoparticles. Russian Chemical Bulletin, **54**, 827–852 (2005). DOI: 10.1007/s11172-005-0331-3

[11] Alivisatos A. P.: Semiconductor clusters, nanocrystals, and quantum dots. Science, **271**, 933–937 (1996). DOI: 10.1126/science.271.5251.933

[12] Link S., El-Sayed M. A.: Shape and size dependence of radiative, non-radiative and photothermal properties of gold nanocrystals. International Reviews in Physical Chemistry, **19**, 409–453 (2000).

[13] Burda C., Chen X., Narayanan R., El-Sayed M. A.: Chemistry and properties of nanocrystals of different shapes. Chemical Reviews, **105**, 1025–1102 (2005). DOI: 10.1021/cr030063a

[14] Medintz I. L., Uyeda H. T., Goldman E. R., Mattoussi H.: Quantum dot bioconjugates for imaging, labelling and sensing. Nature, **4**, 435–446 (2005). DOI: 10.1038/nmat1390

[15] Huang H., Dorn A., Bulovic V., Bawendi M. G.: Electrically driven light emission from single colloidal quantum dots at room temperature. Applied Physics Letters, **90**, 23110–23111 (2007). DOI: 10.1063/1.2425043

[16] Rao C. N. R., Govindaraj A., Vivekchand S. R. C.: Inorganic nanomaterials: Current status and future prospects. Annual Reports on the Progress of Chemistry, Section A, **102**, 20–45 (2006). DOI: 10.1039/b516174f

[17] Li Y., Rizzo A., Cingolati R., Gigli G.: Bright white-light-emitting device from ternary nanocrystal composites. Advanced Materials, **18**, 2545–2548 (2006). DOI: 10.1002/adma.200600181

[18] Versavel M. Y., Haber J. A.: Lead antimony sulfides as potential solar absorbers for thin film solar cells. Thin Solid Films, **515**, 5767–5770 (2007). DOI: 10.1016/j.tsf.2006.12.077

[19] Versavel M. Y., Haber J. A.: Structural and optical properties of amorphous and crystalline antimony sulfide thin-films. Thin Solid Films, **515**, 7171–7176 (2007). DOI: 10.1016/j.tsf.2007.03.043

[20] Roy B., Chakraborty B. R., Bhattacharya R., Dutta A. K.: Electrical and magnetic properties of antimony sulphide (Sb_2S_3) crystals and the mechanism of carrier transport in it. Solid State Communications, **25**, 937–940 (1978). DOI: 10.1016/0038-1098(78)90306-X

[21] Chokalingam M. J., Nagaraja Rao K., Rangarajan R., Suryanarayana C. V.: Studies on sintered photoconductive layers of antimony trisulphide. Journal of Physics D: Applied Physics, **3**, 1641–1644 (1970). DOI: 10.1088/0022-3727/3/11/311

[22] Arivuoli D., Gnanam F. D., Ramasamy P.: Growth and microhardness studies of chalcogenides of arsenic, antimony and bismuth. Journal of Materials Science Letters, **7**, 711–713 (1988). DOI: 10.1007/BF00722076

[23] Wu Q-S., Zhang G-X., Ding Y-P.: Soft-template synthesis and optical properties of Sb_2S_3 semiconductor quasi-nanospheres. Journal of Nanoparticle Research, **8**, 737–742 (2006). DOI: 10.1007/s11051-005-4965-8

[24] Taylor J. R., Fang M. M., Nie S.: Probing specific sequences on single DNA molecules with bioconjugated fluorescent nanoparticles. Analytical Chemistry, **72**, 1979–1986 (2000). DOI: 10.1021/ac9913311

[25] Wu J. S., Dhara S., Wu C. T., Chen K. H., Chen Y. F., Chen L. C.: Growth and optical properties of self-organized Au_2Si nanospheres pea-podded in a silicon oxide nanowire. Advanced Materials, **14**, 1847–1850 (2002).
DOI: 10.1002/adma.200290017

[26] Hu Y., Chen J., Chen W., Lin X., Li X.: Synthesis of novel nickel sulfide submicrometer hollow spheres. Advanced Materials, **15**, 726–729 (2003).
DOI: 10.1002/adma.200304687

[27] Carotenuto G., Martorana B., Perlo P., Nicolais L.: A universal method for the synthesis of metal and metal sulfide clusters embedded in polymer matrices. Journal of Materials Chemisty, **13**, 2927–2930 (2003).
DOI: 10.1039/b310898h

[28] Mehrotra R. C., Gupta V. D., Chatterjee S.: A study of alkylthioantimonites $Sb(SR)_3$. Australian Journal of Chemistry, **21**, 2929–2932 (1968).

[29] Hines M. A., Guyot-Sionnest P.: Synthesis and characterization of strongly luminescing ZnS-capped CdSe nanocrystals. The Journal of Physical Chemistry, **100**, 468–471 (1996).
DOI: 10.1021/jp9530562

[30] Murray C. B., Norris D. J., Bawendi M. G.: Synthesis and characterization of nearly monodisperse CdE (E = sulfur, selenium, tellurium) semiconductor nanocrystallites. Journal of the American Chemical Society, **115**, 8706–8715 (1993).
DOI: 10.1021/ja00072a025

[31] Pigau N.: Structural characterization and optical properties of annealed Sb_2S_3 thin films. Romanian Journal of Physics, **53**, 209–215 (2008).

[32] Vedeshwar A. G.: Optical properties of amorphous and polycrystalline stibnite (Sb_2S_3) films. Journal de Physique III, **5**, 1161–1172 (1995).
DOI: 10.1051/jp3:1995183